



This is a repository copy of *Optimized design of soil reinforcement layout*.

White Rose Research Online URL for this paper:

<https://eprints.whiterose.ac.uk/169234/>

Version: Accepted Version

---

**Article:**

Gonzalez-Castejon, J. and Smith, C.C. [orcid.org/0000-0002-0611-9227](https://orcid.org/0000-0002-0611-9227) (2022) Optimized design of soil reinforcement layout. *Géotechnique*, 72 (6). pp. 486-495. ISSN 0016-8505

<https://doi.org/10.1680/jgeot.19.P.326>

---

© 2021 Institution of Civil Engineers. This is an author-produced version of a paper accepted for publication in *Géotechnique*. Uploaded in accordance with the publisher's self-archiving policy.

**Reuse**

Items deposited in White Rose Research Online are protected by copyright, with all rights reserved unless indicated otherwise. They may be downloaded and/or printed for private study, or other acts as permitted by national copyright laws. The publisher or other rights holders may allow further reproduction and re-use of the full text version. This is indicated by the licence information on the White Rose Research Online record for the item.

**Takedown**

If you consider content in White Rose Research Online to be in breach of UK law, please notify us by emailing [eprints@whiterose.ac.uk](mailto:eprints@whiterose.ac.uk) including the URL of the record and the reason for the withdrawal request.



[eprints@whiterose.ac.uk](mailto:eprints@whiterose.ac.uk)  
<https://eprints.whiterose.ac.uk/>

# Optimized Design of Soil Reinforcement Layout

J. GONZÁLEZ-CASTEJÓN\* AND C.C. SMITH†

The analysis of mechanically stabilised earthworks using geosynthetic reinforcements is typically addressed by means of a limit equilibrium or finite element analysis. However the design of the reinforcement layout and strength is generally specified based on design guidance or on experience. Limit analysis, and in particular Discontinuity Layout Optimization (DLO) presents an alternative for both the analysis and design of reinforced slopes. The current study presents a novel automated approach for determining the optimum layout of reinforcement for any given earthwork geometry. In this paper, a modified formulation of DLO termed Reinforcement Layout and Strength Optimization (RLSO) is presented that is able to find the minimum tensile strength of the reinforcing material and optimal layout required for the stability of the system for a given initial design domain. Examples are given for a slope stability problem and compared with conventional design guidance.

KEYWORDS: reinforced soils; numerical modelling; limit state design/analysis

## INTRODUCTION

Stabilisation of slopes or construction of artificial embankments using geosynthetic reinforcements has been a widely used technique in geotechnical engineering in recent decades. Incorporation of a geosynthetic reinforcement provides the system with an additional tensile strength element that will contribute to the overall stability of the construction. With the widespread use of such systems, there is a clear benefit in optimizing the use of reinforcement materials to maximise efficient resource usage and minimise environmental impact.

Design optimization is an established methodology that is starting to see application in structural engineering practice e.g. [Ye \*et al.\* \(2017\)](#) and is expected to see increasing use across civil engineering in the near future. There has however been limited work in this area in the field of geotechnical engineering. [Ponterosso & Fox \(2000\)](#) used a Genetic Algorithm to enhance the design procedure used in the Highways Agency document [HA 68/94 \(1994\)](#) to generate more optimal layout of reinforcements in slopes. [Kammoun \*et al.\* \(2019\)](#) utilised topology optimization in a limit analysis framework to optimize the soil strength as part of a foundation design system. This paper presents a new automated ultimate limit state (ULS) design procedure utilising linear programming to determine the optimal layout and strength of reinforcement for a wide range of construction profiles and soil types.

## REINFORCED SLOPE ANALYSIS

Conventionally, slope stability analysis is usually tackled using empirical, limit equilibrium (LE) approaches or finite element analysis (FEA). Classical limit equilibrium approaches include:

- Slip circle analyses (e.g. [Bishop, 1955](#))
- Log-spiral approaches (e.g. [Leshchinsky & Smith, 1989](#))

Similarly the design of reinforced slopes and embankments is generally addressed using extended LE (e.g. [Woods & Jewell,](#)

[1990](#), [Jewell \*et al.\*, 1985](#)) or FEA. Alternatively, working stress methods have been proposed by several authors for the design of reinforced soil walls e.g. [Allen & Bathurst \(2015\)](#), [Ehrlich & Mirmoradi \(2016\)](#). In order to account for the presence of reinforcement in a LE analysis, a common approach is to represent the action of the reinforcement by an additional stabilising force due to each element of the reinforcement acting at the point where the reinforcement intersects the assumed failure surface. An aspect which requires additional specific analysis in conventional LE is the possibility that independent slip could occur between the geosynthetic reinforcement and the soil above and below the reinforcement. However LE is unable to capture the different stress-strain behaviour of the soil and the reinforcement and assumes that at failure both materials fully mobilise their peak strengths. To compensate, it is common practice in LE to set a threshold value on the reinforcement strength. Working stress methods are able to overcome these limitations and can represent the differential mobilisation of the peak resistance for each material related to the deformations produced. On the other hand, working stress methods are strongly empirical and do not succeed in creating a general framework for the analysis of mechanically stabilised earth structures.

The previously stated limitations, can potentially be overcome by using FEA generating a fully coupled system, where the deformations are tracked throughout and the geosynthetic reinforcement can move independently within the soil. However FEA usually requires expertise for the use of advanced constitutive models and determination of the factor of safety is less straight forward. Therefore unless the problem requires special in-depth study, limit equilibrium is typically preferred due to its simplicity.

[Clarke \*et al.\* \(2013\)](#) introduced an alternative approach of modelling soil reinforcement using the computational limit analysis procedure Discontinuity Layout Optimisation (DLO) as described by [Smith & Gilbert \(2007\)](#) and [Smith & Gilbert \(2010\)](#). This method utilises optimization techniques to find the critical collapse mechanism for a wide range of geotechnical problems including slopes and reinforced embankments. While [Clarke \*et al.\*](#) modelled soil nails, more recent work by [Smith & Tatari \(2016\)](#) modelled soil reinforcements in the context of embankment stability, and [Xie & Leshchinsky \(2015\)](#) performed a parametric study to manually determine the

Manuscript received . . .

\* University of Sheffield, Department of Civil and Structural Engineering, Sheffield, S1 3JD, UK

† University of Sheffield, Department of Civil and Structural Engineering, Sheffield, S1 3JD, UK (Orcid:0000-0002-0611-9227)

optimal geosynthetic reinforcement density for a reinforced wall under a footing load using DLO.

Although DLO is based on the theory of perfect plasticity and no information about the deformations prior to collapse can be obtained, it possesses some advantages in comparison to conventional LE approaches:

- The ability to directly predict the most critical failure mechanism without the necessity to manually propose and iterate through several mechanisms and select the one with the lowest factor of safety.
- No need to distinguish internal and external stability. The identified critical failure mechanism could e.g. be a rotational failure of a slope or the local rupture of one of the reinforcement elements. Compound failure can also be captured by the model.
- Soil reinforcement interaction is modelled independently on both sides of the reinforcement allowing a broad range of interactions to be modelled including pullout and sliding.
- A threshold can also be applied on the tensile strength of the reinforcement.

Furthermore, since the analysis technique is couched in terms of an optimization process, it is possible to efficiently combine both analysis *and* design aspects into the optimization. Recent work by [Gonzalez-Castejon & Smith \(2018\)](#), presented a formulation termed reinforcement strength optimization (RSO) which can predict the minimum tensile strength necessary for stability of a reinforced slope for a pre-determined reinforcement layout. The current paper presents a significant extension of this latter study and an enhancement of the DLO analysis procedure to provide a new design capability which will be termed here Reinforcement Layout and Strength Optimisation (RLSO). This can predict the optimal layout of reinforcement in addition to its strength based on a initial allowable domain.

This paper will first review conventional design approaches before presenting the new procedure.

## CONVENTIONAL SOIL REINFORCEMENT DESIGN

### Limit Equilibrium

The design of reinforced slopes and embankments is based mainly on limit equilibrium methods assuming two-part wedge analyses (e.g. [Woods & Jewell, 1990](#)), modified circular slip analysis and log-spiral approaches (e.g. [Leshchinsky & Smith, 1989](#)). The presence of reinforcement contributes to the stability of the system by adding a new component to the resisting moment or a horizontal force that improves the force balance in the horizontal direction. It may also contribute to an increased normal stress on a slip-surface and thus an enhanced frictional shear resistance.

To provide a benchmark design, the reinforcement required to stabilise the 70° slope shown in Figure 1a, was determined using the design calculation procedure outlined in [HA 68/94 \(1994\)](#) for a reinforcement design tensile strength of 14.4 kN/m. The solution layout is shown in Figure 1b assuming all given properties are design values and assuming an interface sliding factor of  $\alpha_R = 0.8$ . Full details of the calculation are given in Appendix 1.

## DISCONTINUITY LAYOUT OPTIMISATION (DLO)

### Fundamentals of DLO

DLO ([Smith & Gilbert, 2007](#)) is a computational limit analysis technique that offers an alternative procedure to those based on limit equilibrium or finite element methods to assess the ULS

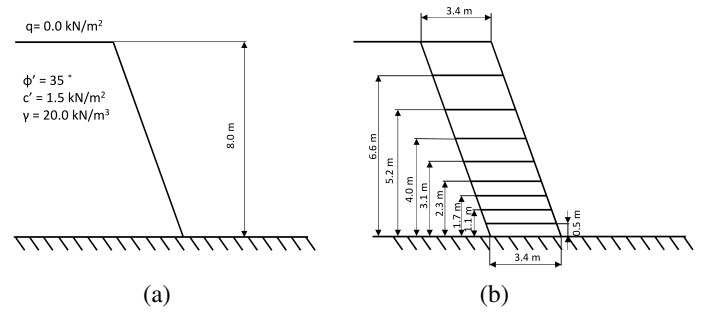


Fig. 1. Hand calculation solution based on [HA 68/94 \(1994\)](#)

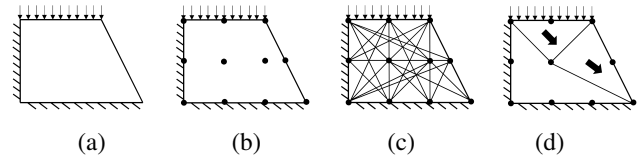


Fig. 2. Stages in DLO procedure: (a) Initial problem definition, surcharge applied to block of soil adjacent to slope crest; (b) discretization of soil block using nodes; (c) interconnection of nodes with potential discontinuities; (d) identification of critical subset of potential discontinuities using optimisation, giving the layout of slip-lines in the critical failure mechanism.

factor of safety of a wide range of geotechnical problems. It provides an automatic general purpose procedure for finding critical upper bound solutions that are generally within a few percent of the true solution. To achieve this, DLO uses a mathematical optimization formulation in the context of the two main assumptions of limit analysis:

- soil is a rigid-perfectly plastic material
- soil obeys an associated flow rule

Qualitatively the DLO procedure can be described by the diagrams shown in Figure 2. In contrast to a FEA approach, DLO discretises the domain using nodes and potential slip-lines connecting those nodes rather than elements. It can therefore be conceptualised as an optimized multi-wedge type of analysis.

The method can be presented in two mathematically equivalent linear programming (LP) forms. One in terms of kinematical parameters (kinematic formulation) and one in terms of force parameters (equilibrium formulation). The latter will be used in this paper as it provides a clearer and more intuitive description of the RLSO algorithm.

### DLO Equilibrium formulation

The basic equations as given by [Smith & Gilbert \(2007\)](#) will be replicated here as a basis for the further development of the RLSO procedure. However it is beyond the scope of this paper to give the full derivation and the reader is referred to [Smith & Gilbert \(2007\)](#) for such details.

For a planar body discretized using  $m$  nodal connections (slip-line discontinuities) and  $n$  nodes the equilibrium form may be stated as follows:

$$\max \lambda$$

subject to:

$$\mathbf{B}^T \mathbf{t} + \lambda \mathbf{f}_L - \mathbf{q} = -\mathbf{f}_D \quad (1)$$

$$\mathbf{N}^T \mathbf{q} \leq \mathbf{g}$$

where  $\mathbf{t}^T = \{t_1^x, t_1^y, t_2^x, t_2^y, \dots, t_n^x, t_n^y\}$  and where  $t_j^x$  and  $t_j^y$  can be interpreted as  $x$  and  $y$  direction equivalent nodal forces acting at node  $j$  ( $j = 1 \dots n$ );  $\mathbf{f}_D$  and  $\mathbf{f}_L$  are vectors containing respectively specified dead and live loads;  $\mathbf{B}^T$  is a suitable  $(2m \times 2n)$  equilibrium matrix,  $\mathbf{N}^T$  is a suitable  $(2m \times 2m)$  yield matrix;  $\mathbf{q}$  is a vector of shear and normal forces acting on discontinuities, i.e.  $\mathbf{q}^T = \{S_1, N_1, S_2, N_2, \dots, N_m\}$ , where  $S_i$  and  $N_i$  represent respectively the shear and normal force acting on discontinuity  $i$  ( $i = 1 \dots m$ );  $\mathbf{g}^T = \{c_1 l_1, c_1 l_1, c_2 l_2, \dots, c_m l_m\}$ , where  $l_i$  and  $c_i$  are respectively the length and cohesive shear strength of discontinuity  $i$

The LP variables are therefore  $t_j^x, t_j^y, S_i, N_i$  and the live load factor  $\lambda$ . The objective is thus to maximize  $\lambda$ , i.e. determine the largest possible live load that can be carried, whilst ensuring that the yield condition is not violated along any potential discontinuity.

While superficially, this formulation resembles the lower bound formulation, it is an upper bound since yield is not checked everywhere within the domain.

The required equilibrium constraint can be written for an individual potential discontinuity  $i$ , orientated at an anti-clockwise angle  $\theta$  to the horizontal, as follows:

$$\mathbf{B}_i^T \mathbf{t}_i + \lambda \mathbf{f}_{Li} - \mathbf{q}_i = -\mathbf{f}_{Di} \quad (2)$$

or, in expanded form as:

$$\begin{bmatrix} \alpha_i & \beta_i & -\alpha_i & -\beta_i \\ -\beta_i & \alpha_i & \beta_i & -\alpha_i \end{bmatrix} \begin{bmatrix} t_A^x \\ t_A^y \\ t_B^x \\ t_B^y \end{bmatrix} + \lambda \begin{bmatrix} f_{Li}^s \\ f_{Li}^n \end{bmatrix} - \begin{bmatrix} S_i \\ N_i \end{bmatrix} = - \begin{bmatrix} f_{Di}^s \\ f_{Di}^n \end{bmatrix} \quad (3)$$

where  $\alpha = \cos \theta$  and  $\beta = \sin \theta$  are direction cosines of the discontinuity, allowing values of  $S$  and  $N$  to be computed on any discontinuity.

The required yield constraint can also be written for a potential discontinuity  $i$  as follows:

$$\mathbf{N}_i^T \mathbf{q}_i \leq \mathbf{g}_i \quad (4)$$

or, in expanded form for the Mohr-Coulomb yield condition as:

$$\begin{bmatrix} 1 & \tan \phi_i \\ -1 & \tan \phi_i \end{bmatrix} \begin{bmatrix} S_i \\ N_i \end{bmatrix} \leq \begin{bmatrix} c_i l_i \\ c_i l_i \end{bmatrix} \quad (5)$$

noting that here tensile forces are taken as positive.

It should be noted that for any given solution,  $S_i$  and  $N_i$  are non-unique except in yielding regions.

## MODELLING SOIL REINFORCEMENT IN DLO

### Principles of the model

Clarke *et al.* (2013) proposed an extended model implemented in DLO able to represent both geosynthetic reinforcements and soil nail reinforcement. Failure could occur either by bending, tensile or compressive rupture, controlled by three parameters. In the current paper only the parameters relevant to planar flexible reinforcement are modelled as follows:

- Reinforcement is modelled using a one dimensional element with a finite tensile strength, zero compressive strength and zero flexural strength.

- Slip-lines can only cross the reinforcement at a node.
- Slip can occur independently above and below reinforcement. There is thus a continuity of normal stresses across the reinforcement but there may be a discontinuity of shear stresses. Any difference results in a change in tension in the reinforcement itself.
- Soil reinforcement can freely move/bend along its full length including the ends.
- The shear strength of the soil/reinforcement interface may be lower than the shear strength of the adjoining soil by a factor  $\alpha_R$ .

Figure 3 shows a section of reinforcement within the soil to illustrate the mechanics of the soil-reinforcement interaction and the corresponding variables which now have independent values above (upper surface,  $u$ ) and below (lower surface,  $l$ ) the reinforcement. Based on the previously stated assumptions the following expressions can be deduced:

$$T_A + S_u = T_B + S_l \quad (6)$$

$$N_u = N_l \quad (7)$$

$$S_u \leq \alpha_R (N_u \tan \phi + c'l) \quad (8)$$

$$S_l \leq \alpha_R (N_l \tan \phi + c'l) \quad (9)$$

$$T_A \leq R_T \quad (10)$$

$$T_B \leq R_T \quad (11)$$

Equation 6 and equation 7 express discontinuity in soil forces parallel to the reinforcement and continuity normal to it respectively, where  $T_A$  and  $T_B$  are the tensile forces within the reinforcement at nodes  $A$  and  $B$ ,  $S_u, S_l$  indicate the tangent forces acting on the upper and lower part of the reinforcement respectively.  $R_T$  is the maximum tensile force of the reinforcement.

### Implementation in DLO formulation

For discontinuities along a reinforcement element, equation 3 is now extended to equation 12 to include equilibrium independently above and below the reinforcement respectively:

$$\begin{bmatrix} \alpha_i & 0 & \beta_i & 0 & -\alpha_i & 0 & -\beta_i & 0 \\ -\beta_i & 0 & \alpha_i & 0 & \beta_i & 0 & -\alpha_i & 0 \\ 0 & \alpha_i & 0 & \beta_i & 0 & -\alpha_i & 0 & -\beta_i \\ 0 & -\beta_i & 0 & \alpha_i & 0 & \beta_i & 0 & -\alpha_i \\ 0 & 0 & 0 & 0 & 0 & 0 & 0 & 0 \\ 0 & 0 & 0 & 0 & 0 & 0 & 0 & 0 \end{bmatrix} \begin{bmatrix} t_A^x \\ t_A^y \\ t_B^x \\ t_B^y \\ t_A^x \\ t_A^y \\ t_B^x \\ t_B^y \end{bmatrix} + \lambda \begin{bmatrix} f_{Li}^s \\ f_{Li}^n \\ f_{Li}^s \\ f_{Li}^n \\ 0 \\ 0 \end{bmatrix} - \begin{bmatrix} 1 & 0 & 0 & 0 & 0 & 0 \\ 0 & 1 & 0 & 0 & 0 & 0 \\ 0 & 0 & 1 & 0 & 0 & 0 \\ 0 & 0 & 0 & 1 & 0 & 0 \\ 0 & 1 & 0 & -1 & 0 & 0 \\ 1 & 0 & -1 & 0 & -1 & 1 \end{bmatrix} \begin{bmatrix} S_{iu} \\ N_{iu} \\ S_{il} \\ N_{il} \\ T_A \\ T_B \end{bmatrix} = - \begin{bmatrix} f_{Di}^s \\ f_{Di}^n \\ f_{Di}^s \\ f_{Di}^n \\ 0 \\ 0 \end{bmatrix} \quad (12)$$

Equation 5 is now extended to the form in Equation 13 to include the reinforcement variables into the yield condition:

$$\begin{bmatrix} 1 & \alpha_R \tan \phi_i & 0 & 0 & 0 & 0 \\ -1 & \alpha_R \tan \phi_i & 0 & 0 & 0 & 0 \\ 0 & 0 & 1 & \alpha_R \tan \phi_i & 0 & 0 \\ 0 & 0 & -1 & \alpha_R \tan \phi_i & 0 & 0 \\ 0 & 0 & 0 & 0 & 1 & 0 \\ 0 & 0 & 0 & 0 & -1 & 0 \\ 0 & 0 & 0 & 0 & 0 & 1 \\ 0 & 0 & 0 & 0 & 0 & -1 \end{bmatrix} \begin{bmatrix} S_{iu} \\ N_{iu} \\ S_{il} \\ N_{il} \\ T_A \\ T_B \end{bmatrix} \leq \begin{bmatrix} \alpha_R c_i l_i \\ \alpha_R c_i l_i \\ \alpha_R c_i l_i \\ \alpha_R c_i l_i \\ R_T \\ R_C \\ R_T \\ R_C \end{bmatrix} \quad (13)$$

where  $R_C$  is the reinforcement compressive strength. For flexible reinforcement this is normally assumed to be zero.

The set of equations 12 represent the equilibrium condition at each slip-line independently above and below the reinforcement element also including the conditions expressed in equations 6 and 7, i.e. continuity of forces in the normal direction and discontinuity in the shear direction. Consequently the vectors of live and dead forces have been expanded, padding with zeros since external loads are not assumed to be applied directly onto the reinforcement in this analysis and the reinforcement is assumed to be weightless. This formulation mirrors conventional LE reinforced soil analysis when only shear interaction with the reinforcement is modelled, and inherently models the effect of any increased normal stresses on a slip-surface due to the reinforcement.

The analyses presented in the subsequent part of this paper were undertaken using the implementation of DLO in the LimitState:GEO software or in a specifically coded MATLAB implementation of the RLSO procedure. Both adopted the preceding reinforced soil DLO formulation, and used the MOSEK solver (Mosek, 2006).

#### Illustrative example

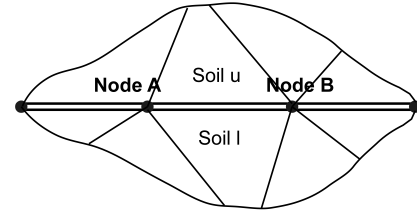
The way DLO is formulated allows it to identify the most critical collapse scenario depending on the characteristics of the problem, simultaneously evaluating possible internal rupture of the reinforcement, front and back end pull-out failure or compound failure of the system. The factor of safety calculated will be therefore the lowest one. Mechanisms with a higher factor of safety can be obtained by manually restricting the problem.

Figure 4 represents a deliberately narrow schematic geometry designed to illustrate a variety of soil-reinforcement interactions during slope failure. Four reinforcement layers (black lines) are modelled with no fixity to the model boundaries. For illustrative purposes, Layers 1, 2 and 4 are modelled with rupture strengths sufficient to prevent yield and Layer 3 is modelled with a lower rupture strength that will result in yield. It can be seen how Layer 1 plays no significant part in the failure mechanism, being fully embedded in the failure wedge. The left hand end of Layer 2 is being pulled out of the underlying soil body, Layer 3 is yielding in tension thus causing a plastic failure of the reinforcement, while the soil wedge is sliding around the right hand end of Layer 4 whose left end remains fixed in the underlying soil layer (front end pullout).

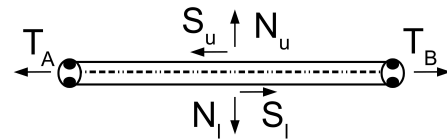
#### Validation

In order to validate the modelling methodology, a reinforced slope problem was modelled using DLO and compared with a limit equilibrium solution by Leshchinsky & Boedeker (1989). The problem comprised a 3 m. slope with an inclination of 2H:5V (68.2°), design soil properties  $\gamma = 18 \text{ kN/m}^3$ ,  $\phi = 35^\circ$ ,  $c' = 0 \text{ kN/m}^2$ . Ten layers of soil reinforcement with a design tensile strength of  $R_T = 5.74 \text{ kN/m}$  were set out at an equal vertical spacing of 0.3 m. The interface soil-reinforcement parameter was defined as  $\alpha_R = 0.8$  with the lengths shown in Figure 5 in order to prevent pull-out failure. This yields a factor of safety of 1.5 using a log-spiral failure mechanism. The solution found using DLO is shown in Figure 5 giving a similar failure mechanism represented by multiple wedges with a factor of safety of 1.42, close to the limit equilibrium solution. The DLO model has been restricted to produce failure mechanisms going through the toe of the embankment as this was the nature of the analysis in the aforementioned reference paper. In order to prevent a shallow surficial local failure on the slope face, an additional narrow layer of stronger ‘facing’

soil has been included in the DLO model. This facing layer has the same frictional properties as the main soil body but with an increased cohesion of  $c' = 2 \text{ kN/m}^2$ . Parametric studies into the effect of this facing layer on global slope failure indicated it would influence the results by  $< 3.5\%$  (values of  $c'$  between 1.8 and 3.0 were modelled, generating a global failure mechanism, and the resulting adequacy factors extrapolated back to a value of 1.38 for  $c' = 0 \text{ kN/m}^2$ ).



(a) Part of soil with reinforcement embedded, showing example slip-line discontinuities meeting at nodes A and B.



(b) Isolated part of reinforcement with internal forces applied.

Fig. 3. Illustrative sketch of the mechanics of soil reinforcement in DLO

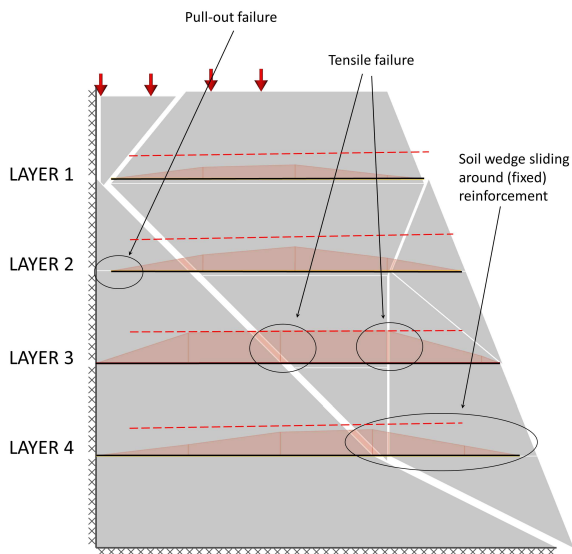


**Fig. 4. Simple model illustrating a compound failure: reinforcement pull-out, plastic failure of reinforcement and soil. Illustrated mechanism includes some deformation to highlight movement of reinforcement (thick black lines). Tensile stresses are plotted relative to the physical level of the reinforcement layer with tensile strength capacity indicated for each layer (horizontal red dashed lines). Note that the reinforcement layers are not attached to the model boundaries.**

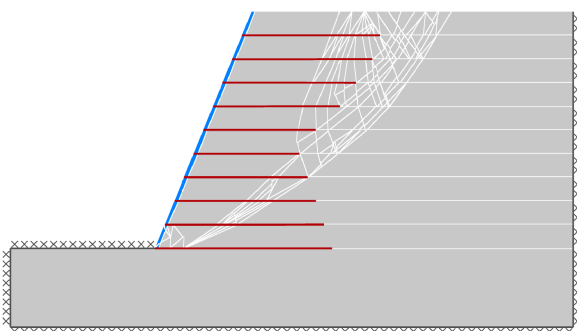


**Fig. 5. Validation of a DLO reinforced slope with strong facing layer using LimitState:GEO**

### REINFORCEMENT STRENGTH OPTIMISATION (RSO).

As a preamble to the development of the full RLSO process, the RSO process (Gonzalez-Castejon & Smith, 2018) will be briefly described. This method is able to determine the maximum global reduction factor on the tensile strength that can be applied to a pre-determined extent of reinforcement and still maintains stability.

This may be formulated as follows:

$$\min \lambda$$

subject to:

$$\mathbf{B}^T \mathbf{t} - \mathbf{q} = -\mathbf{f} \quad (14)$$

$$\mathbf{N}^T \mathbf{q}_s \leq \mathbf{g}_s$$

$$\mathbf{N}^T \mathbf{q}_r \leq \lambda \mathbf{g}_r$$

where the subscripts  $s$  and  $r$  represents the soil and reinforcement respectively and  $\mathbf{f}$  now represents all loading in the system as there is no longer a distinction between live and dead loads.  $\mathbf{g}_r$  therefore represents either  $R_T$  or  $R_C$  as appropriate.

In this case the linear programming solution determines a uniform applied factor to the reinforcement tensile capacity needed in order to carry a given external load. This can be a useful approach for the designer to find the ultimate tensile strength of the reinforcement for a given initial layout and fixed loading. While simple, the above approach has some limitations as follows:

- The tensile strength multiplier  $\lambda$  is applied uniformly to every layer of reinforcement.
- The method requires the designer to pre-determine the layout of the reinforcement system.
- There is no unique information concerning the stresses in the reinforcement unless they are yielding and therefore no definitive information concerning unused pieces of reinforcement. (This non-uniqueness of stresses in non-yielding zones is an intrinsic nature of any limit analysis solution).

### REINFORCEMENT LAYOUT OPTIMIZATION

In order to overcome the above limitations a modified formulation will now be presented termed Reinforcement Layout Optimization (RLO). This is an intermediate stage to achieving combined layout and strength optimization. Rather than seeking a global factor on reinforcement strength, the objective function is modified to seek the minimum volume of reinforcement required to just avoid collapse under the applied loading. If the tensile force per unit width of reinforcement  $T$  is known at any point and acts over a length  $l$  then the volume of reinforcement required  $V$  is given by:

$$V = \frac{Tl}{\sigma_y} \quad (15)$$

where  $\sigma_y$  is the yield stress of the reinforcement material. To minimise the volume in the whole system while not violating yield, a new objective function is introduced into equation 14

$$\min \sum \frac{Tl}{\sigma_y} \quad (16)$$

However, since this is to be summed along each discontinuity containing reinforcement, while the tensile force  $T$  is evaluated at nodes, an alternative averaged equation is used in practice:

$$\min \sum \frac{0.5(T_A + T_B)l_i}{\sigma_{yi}} \quad (17)$$

subject to:

$$\mathbf{B}^T \mathbf{t} - \mathbf{q} = -\mathbf{f} \quad (18)$$

$$\mathbf{N}^T \mathbf{q} = \mathbf{g} \quad (19)$$

where node  $A$  and node  $B$  are at either end of reinforcement element  $i$ .

While the objective is to minimise the total reinforcement volume, the given solution is the one corresponding to the most critical collapse mechanism in terms of energy dissipation, taking into account all possible failure modes.

Here the optimization is undertaken with a maximum limit on the tensile stress  $R_T$  in the reinforcement at any point. In general, the results generated by the method will generate zero or near zero tensile stresses in areas where reinforcement is not required and positive values where it is required. However if  $R_T$  is too low then no solution may be possible. There may also be cases where no value of  $R_T$  can achieve stability. This can be usually observed when the reinforcement spacing is too large and local failures are produced.

In order to qualitatively illustrate how RLO can identify the areas where soil reinforcement is not needed and push them to zero, the problem geometry used in Figure 4 has been analysed but in this case using the same value of  $R_T$  for all layers. The edges of the reinforcements are again modelled unattached to the problem boundaries.

Figure 6 shows the values of the tensile forces in the reinforcement at the nodes based on a standard DLO analysis (solid black lines), together with the forces for the same problem after the application of the RLO procedure (red dashed lines). The failure mechanism after RLO is also shown (white lines) which for this specific example coincides with the mechanism found using standard DLO. As depicted, the tensile forces in the lengths of reinforcement that are not necessary for stability have been pushed to zero. Based on this, the designer can remove the unnecessary parts obtaining an optimised reinforcement layout.

Alternatively this stage can be automated by adopting a post processing stage that removes all elements for which  $0.5(T_A + T_B) < \epsilon R_T$  where  $\epsilon$  is a suitable small number.

In the cases studied in this paper, values of  $\epsilon = 10^{-3}$  were found to work well. Since in practice, tensile reinforcement is laid only in uniform sheets, the remainder of the connected elements are assigned a strength equal to the maximum tensile stress determined in that layer. The full model is then re-run as a standard DLO problem to check that the design is still adequate. If not the post-processing stage is re-run using an increased value of  $\epsilon$ .

### REINFORCEMENT LAYOUT AND STRENGTH OPTIMIZATION

RLO may be used directly with a fixed value of the reinforcement strength  $R_T$  if that is determined by the availability of materials on site (separate strengths for different layers may also be adopted). If, however the optimal reinforcement strength is also required, an additional step is necessary.

Large values of  $R_T$  give the optimiser the greatest degree of freedom and therefore the lowest theoretical volume based on the tensile stresses, after the initial analysis. However, after the post processing determines the lowest reinforcement lengths, it assigns the same tensile strength to all layers, even if they

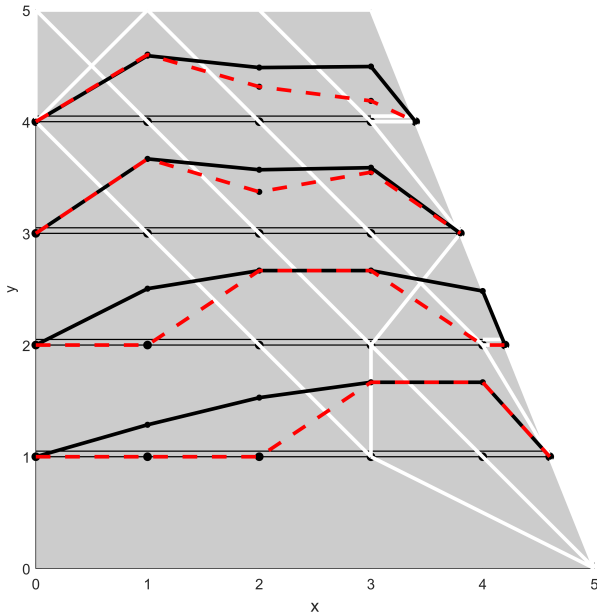


Fig. 6. Comparison of tensile stresses using DLO (solid black lines) and RLO (red dashed lines). Tensile stresses are plotted relative to the physical level of the reinforcement layer.

are only required to carry a lower tensile stress. Hence, the use of large initial value of  $R_T$  can paradoxically result in a larger overall final design volume. It has therefore been found as a general rule for the cases studied by the authors, that if  $R_T$  is established using RSO first and then applied to the RLO procedure, then a near optimal layout is obtained. This will be illustrated later. The combined process is therefore termed Reinforcement Layout and Strength Optimization or RLSO.

#### RLSO DESIGN PROCEDURE

The above calculation procedure may be summarised as follows. :

1. Define an oversized layout of reinforcement using unrealistically long layers of reinforcement, expanding the model boundaries as appropriate. The vertical spacing between reinforcement layers is an input parameter that is to be specified by the user.
2. Assign a nominal value (e.g. 1 kN/m) to the tensile strength  $R_T$  of the reinforcements.
3. Apply the global factor on reinforcement strength (RSO) procedure to determine the minimum tensile strength  $R_{T,min}$  required to carry the external applied load.
4. Use  $R_{T,min}$  as the input value for the limiting tensile capacity for a RLO analysis assuming it is uniformly distributed throughout all the layers
5. Run the RLO optimization and remove any element for which the predicted average tensile force is less than  $\epsilon R_T$ , where  $\epsilon$  is some suitable small value.
6. Validate the solution by running it as a standard DLO problem. The factor  $\lambda$  should come out equal to or just greater than 1.0. If smaller then re-run stage 5 with a larger value of  $\epsilon$ .

For simplicity the described procedure does not include application of global or partial factors of safety which may be pre-applied to relevant parameters.

It is noted that Stages 2-6 may be automated and carried out internally by the software. The procedure only needs user

interaction for Stage 1 and the interpretation of the achieved solution.

#### EXAMPLE AND GUIDELINES FOR THE DESIGN

The RLSO procedure was applied to the design example presented in Figure 1 and the results are given in Figure 7. The same number of layers, vertical spacing, soil and reinforcement properties were adopted. The first three figures, represent the same analysis performed with different nodal spacings after RLSO, where the RSO component of the procedure gave an optimised required value  $R_{T,min} = 10.0$  kN/m (with slight variation of 3% depending on the nodal spacing). This value is lower than the one used in the hand calculation (14.4 kN/m).

Compared to the HA68/94 design, longer length sections of reinforcement for the upper layers (Figure 7d) are obtained close to the crest of the slope and shorter lengths towards the base of the slope. This mirrors the expected form of the failure mechanism and indicates that the HA68/94 design appears to require an overconservative base reinforcement length due to simplifying assumptions in the analysis.

It can also be seen in Figure 7d that use of the higher strength of 14.4 kN/m allows the solution to achieve shorter lengths. This capability can be used by the designer in order to achieve the most convenient solution depending on the problem addressed and the availability of different tensile strengths and lengths of the reinforcements.

Figure 8 shows an analysis of the variation of the total length and volume per unit width with respect to the available tensile strength of the reinforcement. It can be seen that the total length decreases monotonically and the volume increases monotonically with strength. It can also be seen that the optimal value of strength in terms of lowest volume is that found after RSO (a lower value is not possible, while retaining stability). For the sake of clarity high values of the tensile strength have not been plotted, however the volume keeps on increasing monotonically and the length tends to approximate a plateau after a certain value depending on the problem type as would be expected. The stepped pattern of the graphs, is due to the discrete nature of the method although this could be reduced if smaller steps of the available tensile strength were to be taken.

A parametric study was also performed for different nodal spacings across the reinforcements in order to check that the results do not fluctuate depending on the nodal spacing chosen. Four possible nodal spacings were utilised: 0.5, 0.25, 0.125, 0.0625m, and the variation of the total length can be seen in Figure 9. The total length changes very slightly with respect to the nodal spacing as it can be seen. The factor of safety applied on  $R_T$  has been observed to vary around 7.5% from a spacing of 0.5m to 0.125m whereas the change is negligible for spacings smaller than 0.125. As with conventional DLO, it can be concluded that the effect of nodal spacing should be checked in any analysis.

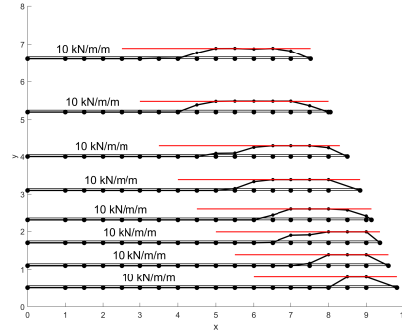
The final optimal reinforcement layout for a strength of 14.4 kN/m (Figure 7d) is shown in Figure 10. This gives a total length of reinforcement of 24m, whereas the hand solution obtained using HA 68/94 (1994) is of 27m, a reduction of around 12% using the same factor of safety for both solutions. The total volume per unit width in each case is 346m<sup>2</sup> and 389m<sup>2</sup> respectively.

A stability analysis and collapse mechanism in terms of a factor of safety on soil strength is given in Figure 10a. The factor obtained is 1.05 indicating an additional 5% margin of safety in the layout, due to the single reinforcement strength value employed.

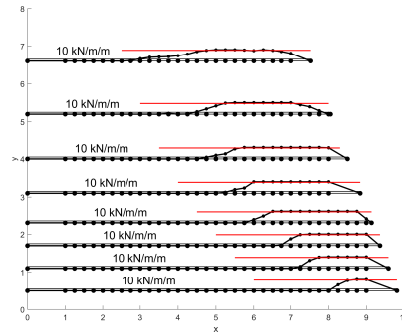
It is also instructive to undertake a stability analysis in terms of a factor of safety on reinforcement tensile strength.

The factor obtained was 1.4 and the corresponding collapse mechanism is shown in Figure 10b. This indicates that this given layout a value of  $R_T = 10.3$  kN/m is sufficient stability and in fact the original RSO value of  $R_T = 10.0$  is close to optimal and that there was little gain in this exercise in utilising the higher value of  $R_T = 14.4$  kN/m.

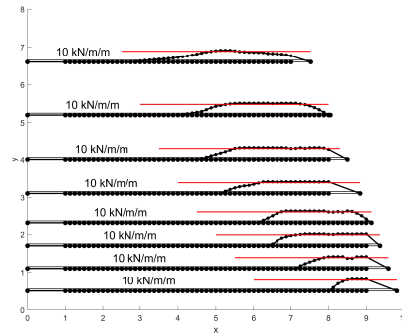
It is noted that both models indicate collapse mechanisms similar in form to those produced by conventional methods such as log-spiral analysis and by physical models e.g. Ba & Benjamin (1990) and Hung *et al.* (2020), for conventional reinforcement layouts.



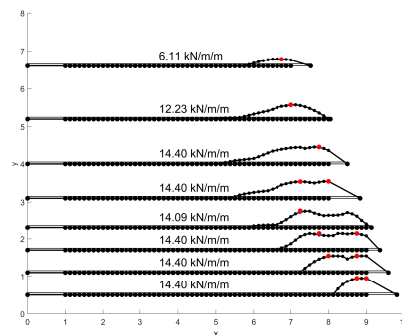
(a) Minimised tensile stresses for a nodal spacing of 0.5 m after RLSO.



(b) Minimised tensile stresses for a nodal spacing of 0.25 m after RLSO.

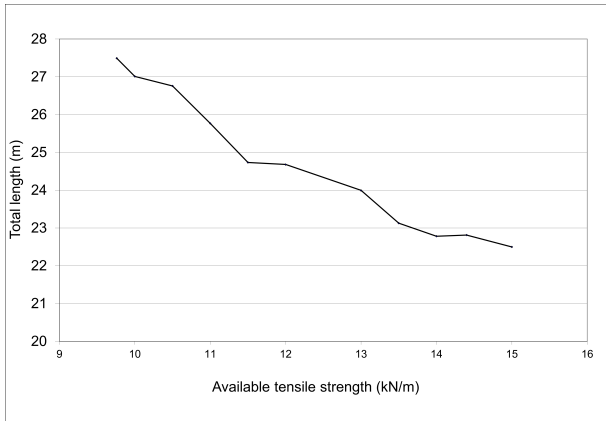


(c) Minimised tensile stresses for a nodal spacing of 0.125 m after RLSO.

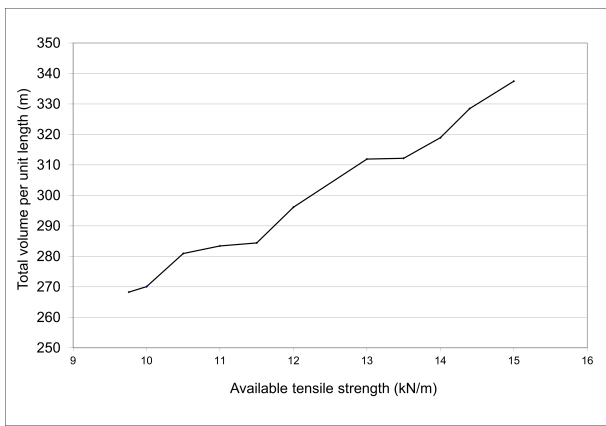


(d) Minimised tensile stresses for a nodal spacing of 0.125 m after RLO.

**Fig. 7.** Different outputs found after using RLO or RLSO with different nodal spacings. Tensile stresses are plotted relative to the physical level of the reinforcement layer with peak values indicated for each layer.



(a) Total length vs. available tensile strength



(b) Total volume per unit width vs. available tensile strength.

**Fig. 8.** Analysis of the variation of the overall length and volume of reinforcement with respect to the tensile strength of the reinforcement, with uniform tensile strength employed in all layers.

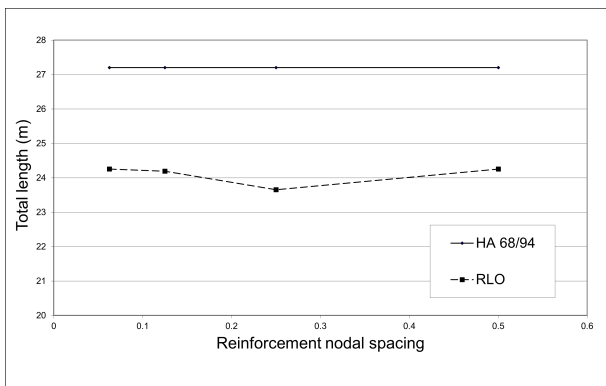
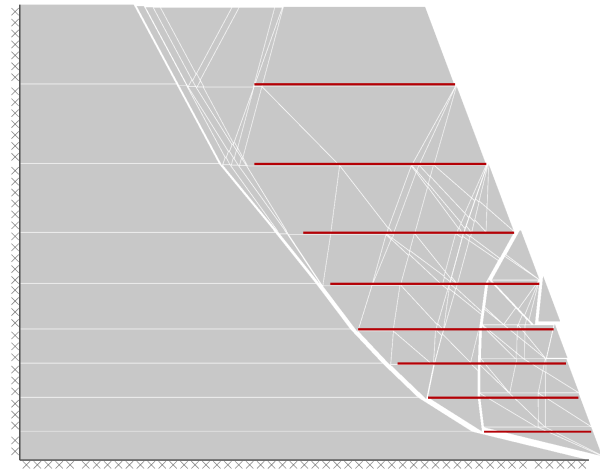
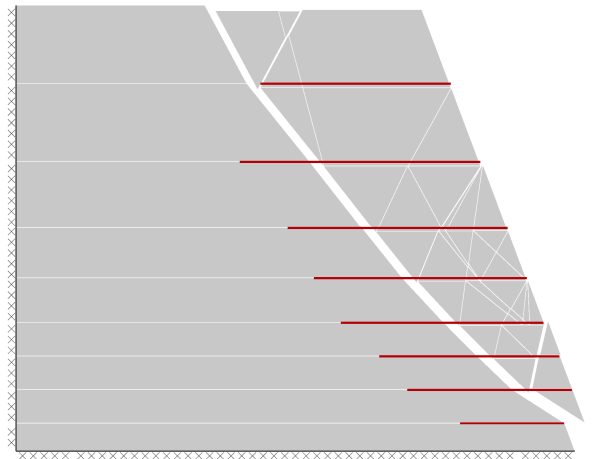


**Fig. 9.** Analysis of the variation of the overall reinforcement length with respect to the DLO nodal spacing along the reinforcement



(a) Factor of safety of 1.05 on soil strength



(b) Failure mechanism for a factor of safety of 1.4 on  $R_T = 14.4$  kN/m

**Fig. 10.** Final adopted solution and failure mechanisms after optimisation of lengths for a tensile strength of 14.4 kN/m

## DISCUSSION

The proposed RLSO procedure has been shown to generate similar but slightly more efficient results compared to the conventional approach given in HA 68/94 (1994) for a simple example slope problem and to generate the expected form of failure mechanisms. This gives confidence in the method and it would not be expected that significantly improved reinforcement layouts could be generated for a simple slope geometry. However the proposed method is likely to prove most valuable for more complex geometries and loading patterns that are difficult to address through hand calculation techniques.

It should be emphasised that the RLSO procedure, like DLO, automatically takes into account all the possible failure mechanisms. There is thus no need for additional separate analyses of e.g. internal and external stability.

RLSO therefore offers a rapid and reliable analysis capability and the engineer can run several simulations in a very short period of time in order to achieve the most suitable combination of tensile strength/optimal layout. Typical run times are only slightly longer than an equivalent DLO analysis of the same geometry and are of the order of seconds to minutes, depending on the nodal distribution adopted.

While RLSO is formulated to minimise the volume of reinforcement utilised, the volume can be taken as a good indicator of the excavation and fill volumes and thus of overall environmental and economic costs. Further work is required to consider how these aspects might be directly optimized.

The procedure does require the engineer to specify potential reinforcement layer elevations, but given there is a practical minimum spacing, this is unlikely to be onerous.

Finally since the solutions have been generated using limit analysis techniques, the design is valid for ULS, but would have to be checked for SLS also and is therefore likely to be of most value in suggesting optimal layouts that can be further refined by the engineer using a more detailed analysis if required.

## CONCLUSIONS

1. A new Reinforcement Strength and Layout Optimization (RLSO) technique has been presented as an automatic method to aid the design of mechanically stabilised geotechnical structures using geosynthetic reinforcement.
2. The RLSO procedure consists of two stages: (i) a Reinforcement Strength Optimization (RSO) stage and (ii) a Reinforcement Layout Optimization (RLO) stage. Both optimisation processes can be run at the same time (when the designer wants to know both optimal strength and layout) or independently. If the layout of reinforcement is known, RSO can be applied to determine the optimal reinforcement strength. Likewise if the tensile strength is known, the RLO algorithm can be used to find the optimised layout.
3. RLSO has been shown to generate a layout similar, but more efficient to an example case of a slope stabilisation based on a standard hand calculation. It is however very flexible and can deal with complex problem geometries.
4. RLSO is also able to predict when reinforcement is not needed at all for the equilibrium of the system and for the case when the system is unstable regardless the amount of reinforcement used. In the latter case an infeasibility error is thrown by the solver.
5. The proposed procedure is rapid and its simplicity allows interactive use by the designer to generate an optimal ULS design. If required this can be further refined

to address working or serviceability state requirements using additional analysis.

## NOTATION

$c$	cohesion
$c'$	drained cohesion intercept
$H$	slope height
$l$	length of discontinuity
$L$	mechanism length
$m$	number of nodal connections
$n$	number of nodes
$N$	normal force on discontinuity
$N$	number of reinforcement layers
$P_{des}$	design tensile strength
$q$	surcharge
$R_C$	reinforcement compressive strength
$R_T$	reinforcement tensile strength
$S$	shear force on discontinuity
$T$	tensile force in reinforcement
$V$	reinforcement volume
$z$	depth below crest
$\mathbf{f}$	external loads
$\mathbf{f}_D$	dead loads
$\mathbf{f}_L$	live loads
$\mathbf{g}$	discontinuity resistance
$\mathbf{q}$	shear and normal forces on discontinuities
$\mathbf{t}$	equivalent nodal forces
$\mathbf{B}^T$	equilibrium matrix
$\mathbf{N}^T$	yield matrix
$\alpha$	direction cosine ( $\cos \theta$ )
$\alpha_R$	soil/reinforcement interface strength factor
$\beta$	direction cosine ( $\sin \theta$ )
$\epsilon$	threshold tolerance factor
$\gamma$	unit weight
$\lambda$	live load factor
$\lambda_p$	non-dimensional pullout factor
$\phi'$	drained angle of shearing resistance
$\theta$	anti-clockwise angle of discontinuity to $x$ -axis

## REFERENCES

- Allen & Bathurst (2015). Improved simplified method for prediction of loads in reinforced soil walls. *J. Geotech. Engng, ASCE* **141**, No. 11.
- Bathurst, R. & Benjamin, D. (1990). Failure of a geogrid-reinforced soil wall. *Transportation Research Record* **1288**, 109–116.
- Bishop, A. W. (1955). The use of the slip circle in the stability analysis of slopes. *Geotechnique* **5**, No. 1, 7–17.
- Clarke, S., Smith, C. & Gilbert, M. (2013). Modelling discrete soil reinforcement in numerical limit analysis. *Canadian Journal of Civil Engineering* **50**, No. 7, 705–715, dx.doi.org/10.1139/cjci-2012-0387.
- Ehrlich, M. & Mirmoradi, S. H. (2016). A simplified working stress design method for reinforced soil walls. *Géotechnique* **10**, 854–863.
- Gonzalez-Castejon, J. & Smith, C. (2018). Optimal design of reinforced slopes. In *Proceedings of the Conference on Numerical Methods on Geotechnical Engineering*.
- HA 68/94 (1994). *Design methods for the reinforcement of highway slopes by reinforced soil and soil nailing techniques*. Highways Agency, London, UK, HA, volume 4 Section 1 Part 4 (HA 68/94).
- Hung, W.-Y., Yang, K.-H., Nguyen, T. S. & Pham, T.-N.-P. (2020). Performance of geosynthetic-reinforced soil walls at failure. *Journal of GeoEngineering* **15**, No. 1, 13–29, doi:10.6310/jog.202003.15(1).2.
- Jewell, R., Paine, N. & Woods, R. (1985). Design methods for steep reinforced embankments. *Polymer grid reinforcement*. Thomas Telford Limited .

Kammoun, Z., Fourati, M. & Smaoui, H. (2019). Direct limit analysis based topology optimization of foundations. *Soils and Foundations* doi:https://doi.org/10.1016/j.sandf.2019.05.003.

Leshchinsky, D. & Boedeker, H. (1989). Geosynthetic reinforced soil structures. *Journal of Geotechnical Engineering* **115**, No. 10.

Leshchinsky, D. & Smith, D. S. (1989). Deep seated failure of a granular embankment over clay: Stability analysis. *Soil and Foundation* **27**, No. 3, 43–57.

Mosek (2006). *The mosek optimization tools manual*. <http://www.mosek.com>, version 4.0 (revision 35) edn. Mosek ApS.

Ponterosso, P. & Fox, D. S. J. (2000). Optimization of reinforced soil embankments by genetic algorithms. *International journal for numerical and analytical methods in geomechanics* **24**, 425–433.

Smith, C. & Gilbert, M. (2007). Application of discontinuity layout optimization to plane plasticity problems. *Royal Society A: Mathematical, Physical and Engineering* **463**, 2461–2484, doi:10.1098/rspa.2006.1788.

Smith, C. C. & Gilbert, M. (2010). *Advances in computational limit state analysis and design*. pp. 119–128, doi:10.1061/41095(365)8.

Smith, C. C. & Tatari, A. (2016). Limit analysis of reinforced embankments on soft soil. *Geotextiles and Geomembranes Journal* **44**, No. 4, 504–514, doi:10.1016/j.geotexmem.2016.01.008.

Woods, R. & Jewell, R. (1990). A computer design method for reinforced soil structures. *Geotextiles and Geomembranes*, No. 9, 233–259.

Xie, Y. & Leshchinsky, B. (2015). MSE walls as bridge abutments: Optimal reinforcement density. *Geotextiles and Geomembranes* **43**, No. 2, 128–138.

Ye, J., Shepherd, P., He, L., Gilbert, M., Davison, B., Tyas, A., Gondzio, J., Weldeyesus, A. & Fairclough, H. (2017). Computational layout design optimization of frame structures. In *Proceedings of the IASS Annual Symposium 2017*.

ACKNOWLEDGMENTS

The authors wish to acknowledge the support of the European Commission via the Marie Skłodowska-Curie Innovative Training Networks (ITN-ETN) project TERRE 'Training Engineers and Researchers to Rethink geotechnical Engineering for a low carbon future (H2020-MSCA-ITN-2015-675762) and the support of the University of Glasgow and LimitState Ltd.

APPENDIX 1: DESIGN TO HA/68/94

The following provides a brief summary of the HA 68/94 (1994) design process used in this paper. A reinforced slope of height  $H$ , fill unit weight  $\gamma$ , design soil strength parameters  $c'$ ,  $\phi'$  and crest surcharge  $q$ , is analysed using a simple two part wedge mechanism. The inter-wedge boundary is taken as vertical and assumed to be smooth. The lower wedge intersects the toe of the slope. From a search of these mechanisms the critical mechanism that requires the greatest horizontal reinforcement force  $T_{max}$  is identified. This defines the length  $L_T$  of the mechanism intersecting the slope crest. Additionally the  $T_{ob}$  mechanism that defines the length  $L_B$  required for the reinforcement zone at the base is determined from an analysis that assumes the reinforced zone behaves as a monolithic retaining wall.

The steps to follow for the design can be summarised as follows:

- Perform iterative calculations to find out the value of  $T_{max}$ .
- Choose a value for the design tensile strength  $P_{des}$  and obtain the number of layers  $N$  using the following expression:

$$N = \frac{T_{max}}{P_{des}} \quad (20)$$

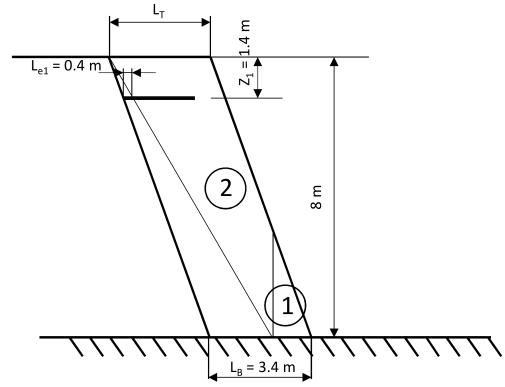


Fig. 11. Simple sketch representing the two part wedge mechanism.

Table 1. Design lengths and depths according to HA 68/94

Layer (top-down)	Depth (m)	Length (m)	Pullout length (m)
1	1.4	3.4	0.4
2	2.8	3.4	0.2
3	4.0	3.4	0.1
4	4.9	3.4	0.1
5	5.7	3.4	0.1
6	6.3	3.4	0.1
7	6.9	3.4	0.1
8	7.5	3.4	0.1

- Obtain the necessary length ( $L_{ei}$ ) to prevent pull-out failure of layer  $i$  (located at depth  $z_i$  below the crest level) using the following expressions:

$$L_{ei} = \frac{P_{des}}{\lambda_p(\sigma'_{vi} \tan \phi' + c')} \quad (21)$$

$$z_1 = 0.5z_2 \quad (22)$$

and for  $i > 1$ ,

$$z_i = H' \sqrt{\frac{i-1}{N}} \quad (23)$$

where  $H' = H + q/\gamma$ ,  $\lambda_p$  is a non-dimensional pull-out factor taken as  $\lambda_p = 2\alpha_R$  and  $\sigma'_v$  is the effective vertical stress at the soil-reinforcement interface.

- Based on the  $T_{max}$  and  $T_{ob}$  mechanisms, obtain  $L_B$  and  $L_T$  (Figure 11). The geometry that defines the mechanism can be found in tables together with the  $L_B$  distance.
- Set out the rest of the layers according to the geometry defined by  $L_T$  and  $L_B$  and the computed reinforcement depths  $z_i$ .

It should be noted that for the sake of simplicity the two part wedge mechanism shown in Figure 11 was assumed to have a cohesion intercept  $c'$  of zero to facilitate use of the design tables in HA 68/94 (1994). However the  $c'$  value was used in equation 21, but has little effect on the calculated pull-out lengths. Table 1 represents the final layout obtained for the previous example using values  $P_{des} = 14.4$  kN/m,  $T_{max} = 113$  kN/m,  $N = 8$ ,  $L_T = 3.4$  m,  $L_B = 3.4$  m.

LIST OF TABLES

- 1 Design lengths and depths according to HA 68/94 11

## LIST OF FIGURES

1	Hand calculation solution based on HA 68/94 (1994) . . . . .	2
2	Stages in DLO procedure: (a) Initial problem definition, surcharge applied to block of soil adjacent to slope crest; (b) discretization of soil block using nodes; (c) interconnection of nodes with potential discontinuities; (d) identification of critical subset of potential discontinuities using optimisation, giving the layout of slip-lines in the critical failure mechanism. . . . .	2
3	Illustrative sketch of the mechanics of soil reinforcement in DLO . . . . .	4
4	Simple model illustrating a compound failure: reinforcement pull-out, plastic failure of reinforcement and soil. Illustrated mechanism includes some deformation to highlight movement of reinforcement (thick black lines). Tensile stresses are plotted relative to the physical level of the reinforcement layer with tensile strength capacity indicated for each layer (horizontal red dashed lines). Note that the reinforcement layers are not attached to the model boundaries. . . . .	4
5	Validation of a DLO reinforced slope with strong facing layer using LimitState:GEO . . . .	5
6	Comparison of tensile stresses using DLO (solid black lines) and RLO (red dashed lines). Tensile stresses are plotted relative to the physical level of the reinforcement layer. . . . .	7
7	Different outputs found after using RLO or RLSO with different nodal spacings. Tensile stresses are plotted relative to the physical level of the reinforcement layer with peak values indicated for each layer. . . . .	8
8	Analysis of the variation of the overall length and volume of reinforcement with respect to the tensile strength of the reinforcement, with uniform tensile strength employed in all layers. .	9
9	Analysis of the variation of the overall reinforcement length with respect to the DLO nodal spacing along the reinforcement . . . . .	9
10	Final adopted solution and failure mechanisms after optimisation of lengths for a tensile strength of 14.4 kN/m . . . . .	9
11	Simple sketch representing the two part wedge mechanism. . . . .	11